Modeling of Brain Tissue Retraction Using Intraoperative Data

Hai Sun[1], Francis E. Kennedy[1], Erik J. Carlson[1], Alex Hartov[1], David W. Roberts[2], and Keith D. Paulsen[1,2]

[1] Thayer School of Engineering, Dartmouth College, Hanover, NH 03755, USA
{Hai.Sun, Francis.E.Kennedy, Erik.J.Carlson, Alex.Hartov, Keith.D.Paulsen}@Dartmouth.edu
[2] Dartmouth Hitchcock Medical Center, Lebanon, NH 03766, USA
David.W.Roberts@Hitchcock.org

Abstract. We present a method for modeling tissue retraction during image-guided neurosurgery. A poroelastic brain model is driven by the stereoscopically-measured motion of a retractor to produce a full volume displacement field, which is used to update the preoperative MR images. Using the cortical surface surrounding the retractor as an independent evaluative landmark, we show that our approach is capable of capturing approximately 75% of the cortical deformation during tissue retraction.

1 Introduction

During neurosurgery, the surgeon often employs retractors to intentionally deform the brain tissue in order to gain access to deeper structures. Although the retraction of brain parenchyma during surgery is common, detailed studies of the effects of retraction on tissue are few [1]. Existing simulations are largely limited to qualitative descriptions of the retraction process [2] and are not capable of producing an accurate estimate of the mechanical impact on the parenchyma.

Computational brain models have proven to be powerful in compensating for brain shift [3,4,5], but their success has been largely limited to the initial tissue response to the craniotomy and dural opening. Miga et al. proposed a strategy for digitizing the motion of the retractor and the volume of the resection cavity in order to incorporate these changes into a brain model [6]. In their initial attempt, the intraoperative data were only qualitatively estimated based on preoperative images due to difficulty in tracking surgical tools and the brain surface during surgery. Using porcine subjects, Platenik et al. [7] demonstrated that their brain deformation model is capable of capturing 75% - 80% of the tissue motion generated during interhemispheric retraction.

In order to accurately model the retraction of a human brain, we employ an intraoperative stereo vision (iSV) system constructed by attaching two CCD cameras to the binocular optics of the operating microscope [8]. We have previously shown that this iSV system is accurate to approximately 1mm [9,10].

The project is funded by the National Institute of Neurological Disorders and Stroke (NINDS, R01-NS33900).

C. Barillot, D.R. Haynor, and P. Hellier (Eds.): MICCAI 2004, LNCS 3217, pp. 225–233, 2004.

Using stereopsis, we have captured the motion of a retractor and continuously monitored the cortical motion during tissue retraction. The measured motion of the retractor is incorporated into the brain model to produce full volume deformation estimates, which are then used to update the preoperative MR (pMR) volume. Using this approach, we have modeled tissue changes both during retraction and after the release of the retractor during a clinical case.

2 Methods

Our technique of modeling tissue retraction involves four basic steps:

1. from preoperative MR scans, generate a finite element mesh of the brain,
2. identify areas of the mesh surface corresponding to both the craniotomy site and the portion of brain tissue under the retractor,
3. track the motion of the retractor using stereopsis,
4. and incorporate the motion of the retractor into the original brain mesh to produce a full volume description of brain deformation.

Each of these steps is described below, and results from one clinical case are presented in the subsequent section.

2.1 Mesh Generation

The modeling process begins with the generation of a computational mesh of the patient's brain using preoperative MR images. The brain is segmented using AnalyzeAVW [1]. The boundary is discretized into triangular patches using the marching cubes algorithm. Custom mesh generation software creates a volumetric mesh consisting of tetrahedral elements [11].

2.2 Sites of Craniotomy and Retraction

This step identifies the portion of the preoperative mesh that corresponds to the sites of both craniotomy and retraction, so that appropriate boundary conditions can be assigned to drive the brain model.

To begin, the coordinate space of the constructed mesh is rigidly registered to the 3-D operating room and the 2-D operating microscope [2] [12]. With these registrations, the coordinates of the surface nodes are first projected into the microscope image. To avoid the inherent ambiguity resulting from this 3-D to 2-D projection, only the surface nodes from the hemisphere of the craniotomy are projected. The boundary of the craniotomy site is manually outlined in the microscope image. The surface nodes that fall within this boundary are identified in the microscope image and hence in the original mesh - this subset of nodes will be referred to as the *craniotomy* nodes.

[1] The software ANALYZE was provided by the Mayo Foundation.
[2] The operating microscope, Model M695, Leica USA, Rockleigh, NJ.

The portion of the mesh underneath the retractor can be identified in the same way. A microscope image acquired immediately prior to the retraction is selected for this estimation. The boundary of the retractor in this image is also outlined. The surface nodes that fall within this second boundary are identified - this subset of nodes will be referred to as the *retractor* nodes, which constitute a subset of the craniotomy nodes.

2.3 Tracking the Retractor

When the surgeon retracts the tissue, a stereo pair of the surgical scene is acquired. Using the technique of stereopsis [8,10], we estimate the shape of the retractor, which is represented by a point cloud, which is transformed into the pMR coordinates using registrations established in the previous section.

To track the retractor motion, we regard the retractor nodes (Section 2.2) as the tool location prior to retraction and the iSV-estimated shape as its location after retraction. Given these two point clouds (both in pMR coordinates), we employ the iterative closest point (ICP) algorithm [13] to simultaneously establish the correspondence between the two and estimate the displacement. The resulting displacement is represented as a set of 3-D translation vectors between each retractor node and its corresponding point on the iSV-estimated shape.

2.4 Brain Modeling

We now use the motion of the retractor to guide a computational model for recovering the full volume deformation. To this end, we have adopted a poroelastic brain model, using Biot's consolidation formulation [14] to represent the brain as an elastically deformable porous medium containing cerebrospinal fluid. The partial differential equations and the finite element method (FEM) for solving this mathematical framework can be found in [3]. The solution to the model equations is obtained by applying known boundary and volumetric forcing conditions and solving for the full volume displacement field and the pressure distribution.

These boundary and volumetric forcing conditions include fluid saturation in the bottom half of the brain, the gravitational direction acquired during surgery, stress-free conditions at the craniotomy and at the highest elevation of the brain, zero normal displacement and zero tangential traction beneath the remainder of the cranium, free flow of fluid at the craniotomy site, and no flow of fluid at the walls corresponding to the rest of the cranium.

The estimated retractor motion is incorporated into the brain model as follows. For each retractor node for which a displacement was estimated via stereopsis, the corresponding finite element equations are precisely enforced by this displacement [5,4]. The output of the brain model is a displacement field over the patient brain, which is then used to update the entire pMR volume [10].

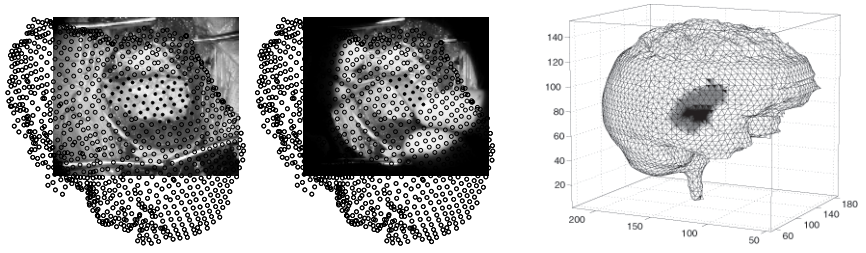

(a) (b) (c)

Fig. 1. Shown, from left to right, are (a) the results of projecting the mesh surface nodes onto the surgical scene, where the nodes within the craniotomy boundary are plotted as asterisks and the others as open circles; (b) a second projection of the mesh surface nodes, where those corresponding to brain tissue underneath the retractor are plotted as asterisks and the others as open circles; and (c) the mesh with the craniotomy nodes colored in lighter gray and the retractor nodes colored in darker gray.

3 Results

In this section, a case study is presented to illustrate how we use the motion of the retractor to model the tissue retraction process. The patient was a 52-year-old female with a right sphenoid wing meningioma. Because of the location of the tumor, the surgeon performed a craniotomy at the right temporal region of the skull and retracted the brain tissue at the craniotomy site in order to gain access to the tumor. Two CCD cameras [3] attached to the operating microscope were used to record the surgical field every 10 seconds during the entire procedure.

Prior to surgery, an MRI scan was obtained, and the cranium segmented. A finite element mesh was generated from the resulting segmented brain and registered to the real-time microscope images, Fig. 1(left and middle), acquired at the start of surgery. The surface nodes that correspond to regions of the craniotomy site (lighter gray) and the tissue underneath the retractor (darker gray) are identified, Fig. 1(right).

Shown in Fig. 2(top) is a stereo pair of the retracted brain tissue. From these images, shapes of the retractor and the cortical surface were estimated. These shapes were overlaid with the preoperative mesh to illustrate the tissue deformation, Fig. 2(bottom). As a result of tissue retraction, the anterior portion of the cortical surface collapsed and the posterior portion of the cortical surface distended. From the retractor nodes in Fig. 1 and the shape of this blade in Fig. 2, the motion of the retractor was estimated using the ICP algorithm. Of the 13 retractor nodes, 8 collapsed and 5 distended. The average displacement of collapsing nodes was 9.23mm, with a maximum of 12.34mm and a minimum

[3] Sony DFW-x700, Resolution $1024(H) \times 768(V)$, Sony Corp., New York, NY, USA

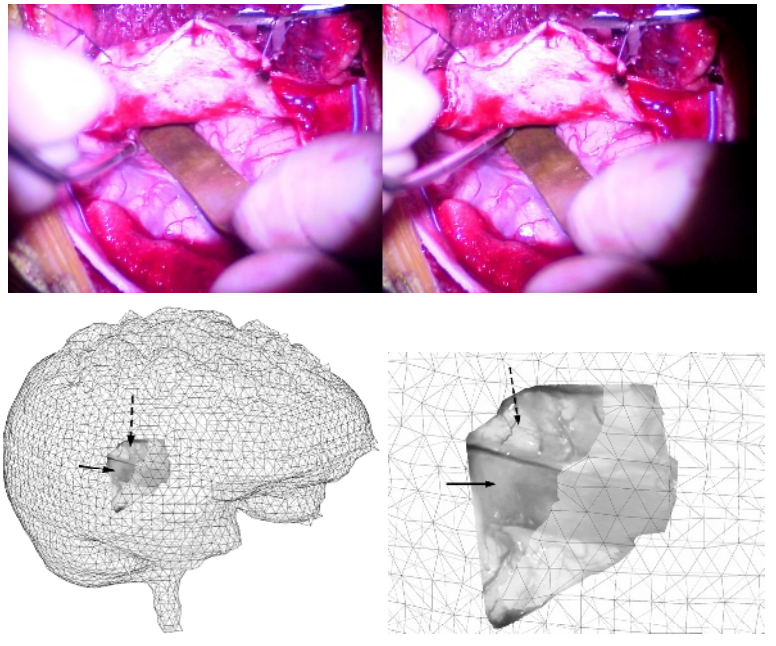

Fig. 2. Shown are: the stereo pair of the retracted brain (top); relative position of the retractor (black arrow) and the deformed cortical surface (dotted arrow) to the preoperative mesh (bottom left) and a close-up view of the same figure (bottom right).

of 4.34mm. The average displacement of distending nodes was 5.42mm, with a maximum of 6.34mm and a minimum of 2.45mm.

The estimated retractor motion was used to guide the brain deformation model, as described in Section 2.4. This model produced a displacement field which was then applied to the pMR volume. Fig. 3 presents the result from this update. The images on the left are the axial slices in the pMR volume with the reconstructed cortical surface (white curves) overlaid. Note the misalignment between the intraoperative and preoperative surfaces. The images on the right display the intraoperative surface overlaid with the updated MR (uMR). Note that these surfaces are now in good alignment.

In order to confirm the viability of our approach in modeling tissue retraction, we compared the model-estimated cortical motion with the same motion captured via stereopsis. Given the accuracy of the iSV system at approximately 1mm [10], we consider the latter estimate as close to the ground truth. The cortical surface surrounding the retractor was used as an evaluative landmark.

To begin, the retractor nodes were subtracted from the craniotomy nodes. The remaining craniotomy nodes, corresponding to the cortical surface surrounding the retractor, were selected for comparison - this set of surface nodes was defined as the *cortical* nodes. As described previously, the brain model had pre-

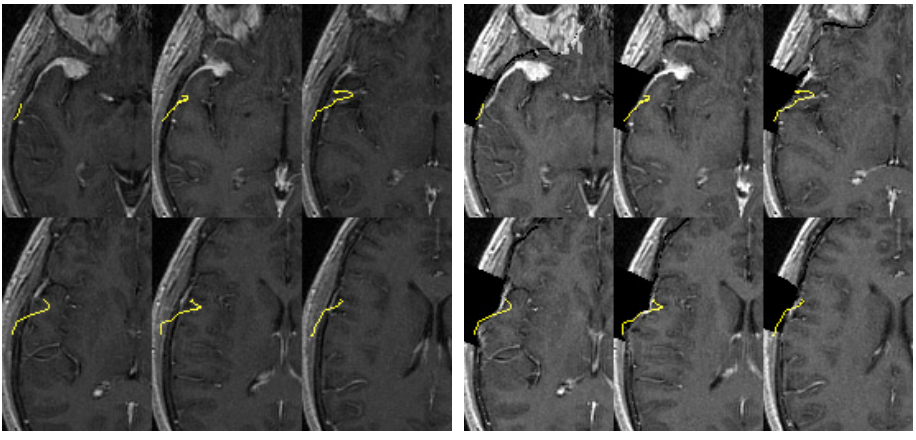

Fig. 3. The retracted cortical surface (white curves) overlaid with axial slices from the pMR volume (left) and the same slices from uMR volume (right).

dicted a displacement for each cortical node. From the stereo pair shown in Fig. 2, the shape of the cortical surface surrounding the retractor was estimated. Using the method described in Section 2.3, the stereo-based estimate of the exposed cortical surface was compared with the corresponding mesh surface, i.e., the cortical nodes, to obtain their displacements. Of 24 cortical nodes, the iSV system estimated that, 15 of those nodes collapsed and 9 distended during retraction. The average displacement of collapsing nodes was 8.76mm, with a maximum of 10.65mm and a minimum of 2.46mm. The average displacement of distending nodes was 4.64mm, with a maximum of 5.64mm and a minimum of 1.83mm.

We next computed, for each cortical node, the absolute difference between the stereo- and model-estimated displacement. The relative difference was determined as the absolute difference divided by the amount of displacement estimated via stereopsis. The final error estimates were cast as the percent capture of tissue motion by subtracting each relative difference from 100 percent. These error estimates were computed in all Cartesian directions (X, Y, Z) and in overall magnitude, Table 1. In this particular case, we have found that our model was capable of capturing approximately 75% of the cortical motion.

In order to further confirm the viability of our approach, we have employed the same strategy to model tissue changes after the release of the retractor. Thirty seconds after the stereo pair in Fig. 2 was acquired, the iSV system recorded another stereo pair shown in Fig. 4 (top). The shape of the cortical surface was estimated using stereopsis and overlaid with the uMR generated during tissue retraction, Fig. 4(bottom left). Note that the cortical surface did not fully recover from the induced tissue deformation. The motion of the retractor nodes was tracked during the recovery phase after blade removal. Of 13 cortical nodes, 4 collapsed and 9 distended after the tissue was released.

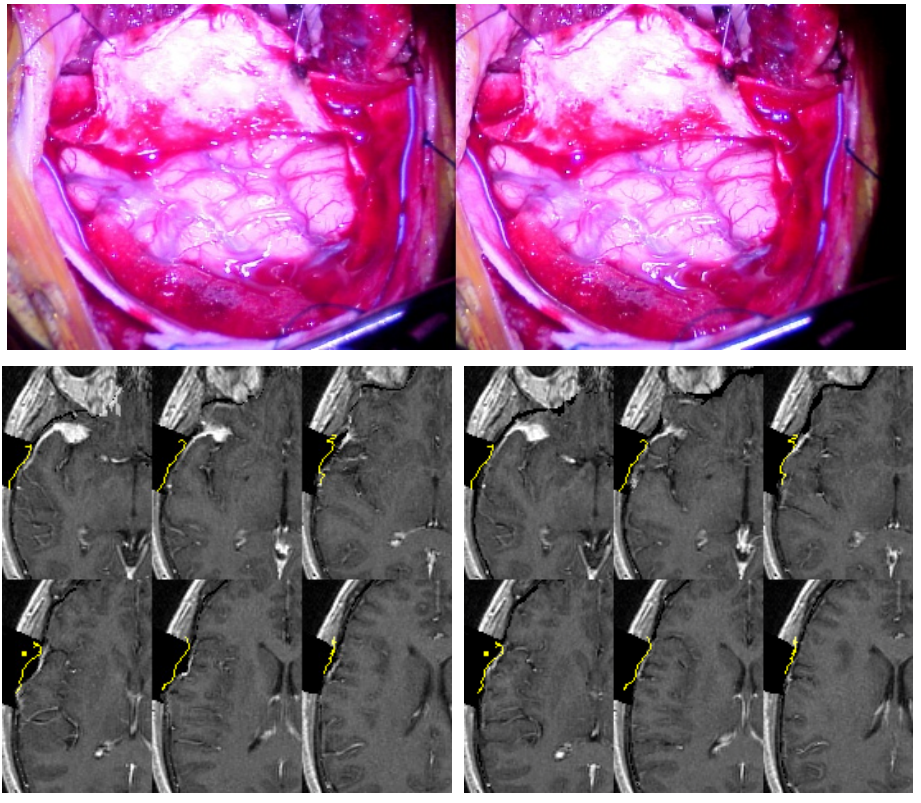

Fig. 4. Stereo pair of the surgical scene taken 30 seconds after the retractor was released (top); The intraoperative cortical surface (white curves) overlaid with axial slices from the uMR volume generated during retraction (bottom left) and the same slices from uMR volume generated after retraction (bottom right).

The average displacement of collapsing nodes was 2.43mm, with a maximum of 4.26mm and a minimum of 1.02mm. The average displacement of distending nodes was 7.32mm, with a maximum of 9.18mm and a minimum of 4.69mm. These retractor nodes displacements were used to guide the brain deformation model for updating the uMR generated during retraction. The images on the right display the current cortical surface overlaid with the uMR generated after 30 seconds during the recovery phase. Note that, compared to the images on the left, the alignment between the intraoperative cortical surface and the surface in the uMR improved as a result of this update. For this modeling step, we also compared the motion of the cortical nodes predicted by the model with the stereo estimation. The model was capable of capturing approximately 72% of the cortical motion during the recovery phase, as shown in Table 2.

Table 1. Percent Capture of Deformation During Retraction

	mean	max	min
X	71.6	97.4	56.7
Y	66.3	89.9	44.3
Z	82.1	98.9	64.4
magnitude	74.8	97.2	53.1

Table 2. Percent Capture of Deformation After Retraction

	mean	max	min
X	69.2	94.3	49.2
Y	78.1	98.4	55.4
Z	65.3	92.1	45.1
magnitude	72.3	96.8	47.9

4 Discussion

We have presented a technique for modeling tissue retraction. By monitoring changes in the surgical field every ten seconds, we have estimated the motion of a retractor and its concomitant cortical surface movement. The retractor motion is then used to drive brain deformation models for updating the preoperative MR volume. Using the cortical surface surrounding the retractor as an independent evaluative landmark, we show that our approach can recover on average approximately 75% of the tissue deformation.

Several extensions and improvements to this work are currently under investigation. First, we plan to further validate our approach through imaging subsurface regions of the brain using co-registered intraoperative ultrasound. Second, in order to improve the modeling results, we plan to test other more sophisticated boundary conditions at the retraction site, in order to produce more realistic tissue motion such as traction along the retractor blade. Finally, we plan to investigate the role of the material properties of the brain in the finite element model. The ability to continuously monitor tissue behavior during the retraction process has the potential of generating more realistic and patient-specific model parameters, which may improve the accuracy of the model estimate.

References

1. Hartkens, T., Hill, D., Castellano-Smith, A., Hawkes, D., Maurer, C., Martin, A., Hall, W., Liu, H., Truwit, C.: Measurement and analysis of brain deformation during neurosurgery. IEEE Transactions on Medical Imaging **22(1)** (2003) 82–92
2. Koyama, T., Okudera, H., Kobayashi, S.: Computer-generated surgical simulation of morpholocial changes in microstructures: Concepts of 'virtual retractor'. Neurosurgery **46(1)** (2000) 118–135
3. Paulsen, K., Miga, M., Kennedy, F., Hoopes, P., Hartov, A., Roberts, D.: A computational model for tracking subsurface tissue deformation during stereotactic neurosurgery. IEEE Transactions on Biomedical Engineering **46** (1999) 213–225
4. Ferrant, M., Nabavi, A., Macq, B., Jolesz, F., Kikinis, R., Warfield, S.: Registration of 3-d intraoperative MR images of the brain using a finite-element biomechanical model. IEEE Transactions on Medical Imaging **20** (2001) 1384–1397
5. Skrinjar, O., Nabavi, A., Duncan, J.: Model-driven brain shift compensation. Medical Image Analysis **6** (2002) 361–373

6. Miga, M., Roberts, D., Kennedy, F., Platenik, L., Hartov, A., , Lunn, K., Paulsen, K.: Modeling of retraction and resection for intraoperative updating of images. Neurosurgery **49** (2001) 75–85
7. Platenik, L., Miga, M., Roberts, D., Lunn, K., Kennedy, F., Hartov, A., Paulsen, K.: In vivo quantification of retraction deformation modeling for updated image-guidance during neurosurgery. IEEE Transactions on Biomedical Engineering **49(8)** (2001) 823–835
8. Sun, H., Farid, H., Rick, K., Hartov, A., Roberts, D., Paulsen, K.: Estimating cortical surface motion using stereopsis for brain deformation models. Medical Image Computing and Computer-Assisted Intervention **2878** (2003) 794–801
9. Sun, H., Roberts, D., Farid, H., Wu, Z., Hartov, A., Paulsen, K.: Cortical surface tracking using a stereoscopic operating microscope. Neurosurgery (in press) (2004)
10. Sun, H., Lunn, K., Farid, H., Wu, Z., Roberts, D., Hartov, A., Paulsen, K.: Stereopsis-driven brain shift compensation. Submitted to:IEEE Transactions on Medical Imaging (2004)
11. Sullivan, J., Charron, G., Paulsen, K.: A three-dimensional mesh generator for arbitrary multiple material domains. Finite Elements in Analysis and Design **25** (1997) 219–241
12. Sun, H., Farid, H., Hartov, A., Lunn, K., Roberts, D., Paulsen, K.: Real-time correction scheme for calibration and implementation of microscope-based image-guided neurosurgery. Proceedings of SPIE Medical Imaging, Visualization, Display, and Image-Guided Procedures **4681** (2002) 47–54
13. Besl, P., McKay, N.: A method for registration of 3-D shapes. IEEE Transactions on Pattern Analysis and Machine Intelligence **14** (1992) 239–256
14. Biot, M.: General theory of three-dimensional consolidation. Journal of Applied Physics **12** (1941) 155–164